Raman-Free, Noble-Gas-Filled Photonic-Crystal Fiber Source for Ultrafast, Very Bright Twin-Beam Squeezed Vacuum

Martin A. Finger,[1,*] Timur Sh. Iskhakov,[1,†] Nicolas Y. Joly,[2,1] Maria V. Chekhova,[1,2,3] and Philip St. J. Russell[1,2]
[1]Max Planck Institute for the Science of Light, Bau 24, 91058 Erlangen, Germany
[2]Department of Physics, University of Erlangen-Nuremberg, Guenther-Scharowsky Strasse 1, Bau 24, 91058 Erlangen, Germany
[3]Physics Department, Lomonosov Moscow State University, Moscow 119991, Russia
(Received 4 May 2015; revised manuscript received 13 August 2015; published 30 September 2015)

We report a novel source of twin beams based on modulational instability in high-pressure argon-filled hollow-core kagome-style photonic-crystal fiber. The source is Raman-free and manifests strong photon-number correlations for femtosecond pulses of squeezed vacuum with a record brightness of ~2500 photons per mode. The ultra-broadband (~50 THz) twin beams are frequency tunable and contain one spatial and less than 5 frequency modes. The presented source outperforms all previously reported squeezed-vacuum twin-beam sources in terms of brightness and low mode content.

DOI: 10.1103/PhysRevLett.115.143602 PACS numbers: 42.50.Dv, 42.50.Ar, 42.50.Lc, 42.65.Lm

Correlated photons and twin beams, among very few accessible nonclassical states of light, are at the focus of modern quantum optics. Their applications in quantum metrology [1–4], imaging [5–7], key distribution [8] and other fields make them the basic resource in photonic quantum technologies. Entangled photon pairs can be generated by parametric down-conversion (PDC) or four-wave mixing (FWM) sources. Depending on the pumping strength, the state emerging at the output of the nonlinear material is called squeezed vacuum (SV) at low photon flux [9], or bright squeezed vacuum (BSV) at high photon flux [10]. The mean field of such states is zero, while the mean energy can approach high values.

In twin-beam SV, there is strong correlation in the photon numbers emitted into the two conjugated beams (called signal and idler). At low photon flux, this simply means that the emitted photons come rarely but always in pairs. For BSV, the numbers of photons emitted into signal and idler beams are very uncertain but always exactly the same. The standard technique for detecting photon-number correlations in this case is to measure the noise reduction factor (NRF), which is the variance of the photon-number difference between the signal and idler channels, normalized to the shot-noise level, i.e., the mean value of the total photon number [11]

$$\mathrm{NRF} = \frac{\mathrm{Var}(N_s - N_i)}{\langle N_s + N_i \rangle}, \quad (1)$$

where N_s, N_i are the photon numbers in the signal and idler modes. NRF is a measure of the reduction of quantum noise below the shot-noise level, which corresponds to $\mathrm{NRF} = 1$.

Fiber-based SV sources are complementary to crystal-based sources and especially interesting because they allow one to engineer temporal correlations while eliminating spatial correlations [12]. The wide flexibility in designing the time-frequency mode structure allows high dimensional temporal Hilbert spaces to be exploited, making such systems promising candidates for more secure quantum cryptography [13] or for high-information-capacity quantum communications, by analogy with multimode states in space [14]. Temporally few-mode systems are a particularly interesting resource in quantum optics, even though addressing and selecting individual frequency modes still presents a challenge [15,16]. Apart from this, fiber-based sources are attractive because of easy manufacturing, high conversion efficiencies due to long optical path lengths, and integrability into optical networks. A major design concern for fibered SV sources is, however, the unavoidable Raman noise [17–20]. There have been many attempts to reduce the deleterious effects of spontaneous Raman scattering (SpRS) on photon correlations, examples being cryogenic cooling of the fiber to 4 K [21], the use of cross-polarized phase matching in birefringent fibers [19], or employing crystalline materials [22]. These techniques suffer, however, from technological difficulties, incomplete suppression of SpRS, or large coupling losses. Another way to reduce SpRS is to generate twin beams spectrally well separated from the pump wavelength. This can be achieved by pumping the fiber in the normal dispersion region, where the generating nonlinear process is FWM [23]. In this regime, the deleterious effects of SpRS are strongly reduced because the sideband spacing is much greater than the Raman shift. Nevertheless, higher-order Raman scattering still corrupts photon-number correlations [18]. Additionally, the wide sideband spacing prevents femtosecond-pulse pumping because signal, idler, and pump photons suffer strong group velocity walk-off [18]. In contrast, pumping the fiber in the anomalous dispersion regime leads to modulational instability (MI), which in the presence of the optical Kerr effect can be phase matched. Under these conditions the signal and idler bands lie very close to the pump frequency, at the same time being broad [Fig. 1(b)] and power dependent (see Supplemental Material [24], Sec. 2). Their proximity to the pump makes them normally difficult to use due to degradation of the lower-frequency sideband by photons Raman scattered from the pump [18–20].

The generation of SV by FWM or MI is described by a Hamiltonian similar to the one for PDC (see Supplemental Material [24], Sec. 1). In such a system the mean number of photons per mode is given by $\langle N \rangle = \sinh^2(G)$, assuming the pump is undepleted [29]. The parametric gain G is proportional to the pump power, the optical path length in the nonlinear material, and the $\chi^{(3)}$ nonlinearity [30]. Despite originating from the same fundamental mechanism, the properties of FWM and MI are substantially different, justifying distinguishing the two processes [18].

In this Letter, we present the first application of gas-filled hollow-core photonic-crystal fiber (PCF) for generating nonclassical states of light. Nonlinearity is provided by argon, which intrinsically avoids SpRS due to its monatomic structure. The fiber is a kagome-lattice hollow core, which has all the essential ingredients for generating ultrafast twin beams. It offers transmission windows several hundred nm wide at moderate losses (typically a few dB/m or less), combined with small values of anomalous group velocity dispersion (GVD) that are only weakly wavelength dependent [31] and can be balanced against the normal dispersion of the filling gas, giving rise to a pressure-dependent zero-dispersion wavelength (ZDW) [32]. This results in turn in large tunability of the signal and idler wavelengths, something that is impossible in solid-core fiber systems even with the help of power-dependent phase matching in the MI regime (see Supplemental Material [24], Sec. 2) [18]. Furthermore, the weak wavelength dependence of the dispersion allows generation of ultra-broadband MI sidebands with widths greater than 50 THz [Fig. 1(b)].

In the setup [Fig. 1(a)], an argon-filled 30-cm-long kagome PCF with a core diameter of 18.5 μm (flat-to-flat) and a core wall thickness of 240 nm was pumped by an amplified Ti:sapphire laser at 800 nm with pulse rate 250 kHz and duration ~300 fs (after a 3.1 nm bandpass filter). Based on an empirical model for the dispersion of kagome PCF (s parameter = 0.03 [33]), these parameters yield a ZDW at 770 nm for a pressure of 75 bar. The pulse energy in the fiber core varied between 140 and 350 nJ, and polarization optics in front of the PCF allowed linear polarized light to be aligned along one eigenaxis of the weakly birefringent fiber. After exiting the PCF the light was collimated with an achromatic lens and the sidebands separated from the pump beam by spectral and spatial filtering. This yielded an overall pump suppression of at least 95 dB. The two sidebands were finally detected using standard silicon PIN photodiodes from Hamamatsu (S3759 and S3399) with ~95% quantum efficiency (protection windows removed), followed by charge sensitive amplifiers, which generate voltage pulses whose area scales with the number of photons per optical pulse. The amplification

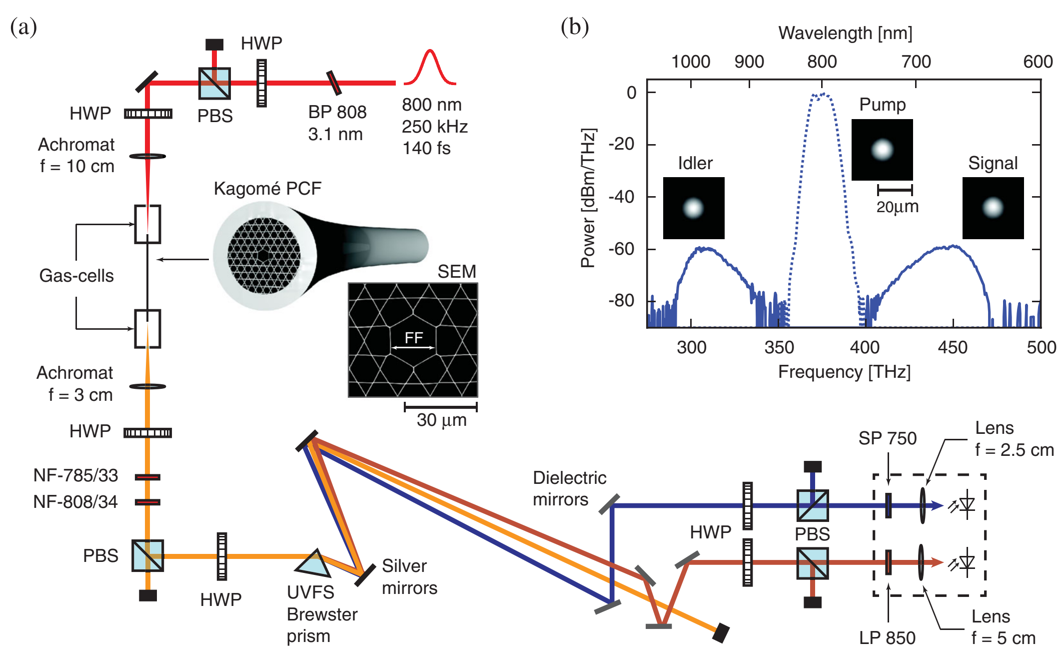

FIG. 1 (color). (a) Setup for twin beam generation and analysis: Bandpass (BP) filter, half-wave plate (HWP), polarizing beam splitter (PBS), notch filter (NF), long-pass (LP) filter, short-pass (SP) filter, scanning electron micrograph (SEM), flat-to-flat (FF) diameter. (b) Modulation instability spectrum at 75 bar and 250 nJ pulse energy measured with an optical spectrum analyzer (OSA/ANDO AQ 6315-E). The dotted curve shows the unfiltered spectrum, while the solid curve shows the spectrum after blocking the pump light with notch filters. The insets show near-field mode profiles, confirming that the light is in the fundamental mode.

factors of the detectors were measured to be (2.096 ± 0.002) pV s/photon for the detector in the high frequency sideband and (2.178 ± 0.004) pV s/photon for the detector in the low frequency sideband. The noise of the photodetectors was determined from the standard deviation of the signals without light. The detector noise amounted to ~600 photons/pulse for the short wavelength sideband and ~650 photons/pulse for the long wavelength sideband. In order to account for the detector response we calibrated the shot-noise level of the system to the coherent state of the laser (see Supplemental Material [24], Sec. 3) [34].

The spectral location of the sidebands was widely tunable by changing the pressure and therefore shifting the ZDW. The overall accessible spectral range (ASR) of the MI sidebands depended on pump power, dispersion (i.e., pressure), and pulse duration. Adjusting the filling pressure from 50 to 96 bar, we were able to tune each sideband by ~80 THz at a fixed pulse energy of 320 nJ, corresponding to a wavelength shift of ~200 nm on the infrared side [see Fig. 2(a)]. Since the pump powers at which we observed nonclassical noise reduction are too small to measure the corresponding spectra directly, we performed nonlinear pulse propagation simulations based on the generalized nonlinear Schrödinger equation. Figure 2(b) shows the pressure dependence of the spectrum at a parametric gain of 4.2, which is in the middle of the parametric gain interval used to observe noise reduction in the system. Note that the ASR limits of the NRF measurement are marked in the figure. Ultimately, the spectral range is limited by the fading nonlinearity at low pressures and by a strongly reduced gain at high pressures due to a larger group-velocity mismatch between the sidebands and the pump. In our case, any spectral cutoff due to group-velocity walk-off is masked by a loss peak in fiber, caused by an anticrossing between the core mode and a cladding resonance [Fig. 2(b)].

Figure 3(a) shows the dependence of NRF on the sum of the mean numbers of detected signal and idler photons at three different pressures. It can be seen that the measured noise in the photon-number difference is ~35% below shot noise, indicating nonclassical correlation of photon numbers between the signal and idler beams. The twin-beam squeezing is observed up to a record value (for squeezed vacuum) of ~2500 photons per mode—almost 3 times brighter than crystal-based sources, which have demonstrated squeezing up to ~900 photons per mode [11]. The measured NRF is in good agreement with loss estimates in the optical channel (see Supplemental Material [24], Sec. 4). The parametric gain was varied within the range 3.9 to 4.6 by increasing the pump power. When the pressure was changed from 70 to 76 bar and the pump pulse energy was kept constant (180 nJ), the signal and idler bands shifted away by ~22 THz. The change in slope for different pressures can be explained by contributions from distinct unmatched modes [11], caused by the unequal frequency dependence of the detection channels. When the number of the unmatched modes increases, the slope becomes steeper due to more uncompensated intensity fluctuations. The accessible pressure range for observation of twin-beam squeezing is limited by a sharp dropoff in the quantum efficiency of the idler silicon photodetector above 1000 nm [see Fig. 2(b)]. In the current configuration, we found the best working pressure to be ~76 bar.

Next we measured the dependence of NRF on loss. In contrast to the normalized Glauber correlation functions, NRF is highly sensitive to losses in the optical channels, the best possible value being $1-\eta$, where η is the quantum efficiency of the optical channel after the PCF [35]. This was tested by monitoring NRF while increasing the loss symmetrically in both channels by adjusting the half-wave plate after the fiber. A linear increase in NRF up to the SNL is observed [Fig. 3(b)], in good agreement with theory. The measured NRF can be further improved by reducing the

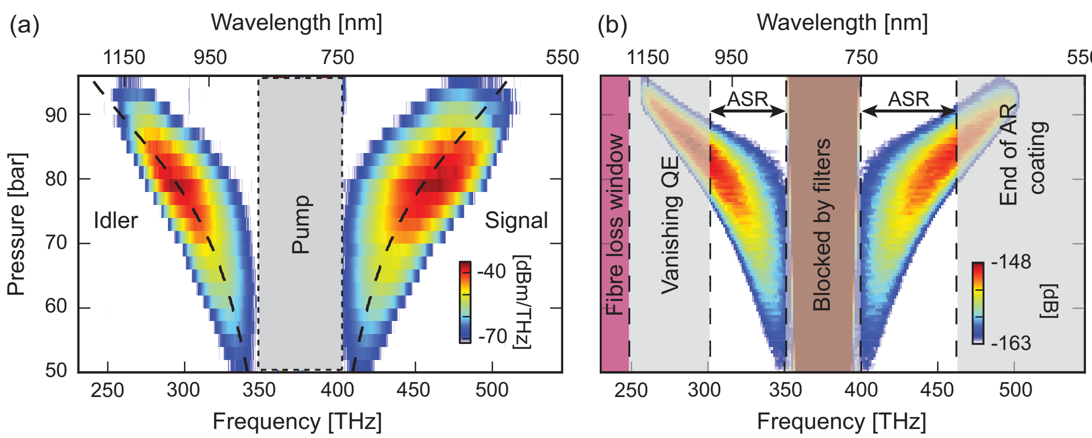

FIG. 2 (color). (a) Measured pressure dependence of the MI sidebands for a constant pump pulse energy of 320 nJ. The spectra were measured with the pump blocked by notch filters. The dashed line marks the locus predicted for perfect phase matching. (b) Simulation of the pressure dependence of the nonclassical light spectra at a parametric gain of 4.2. The accessible spectral range (ASR) for measuring twin-beam squeezing is limited by the quantum efficiency (QE) of the silicon photodiode and by the width of the antireflection (AR) coating on the optical components.

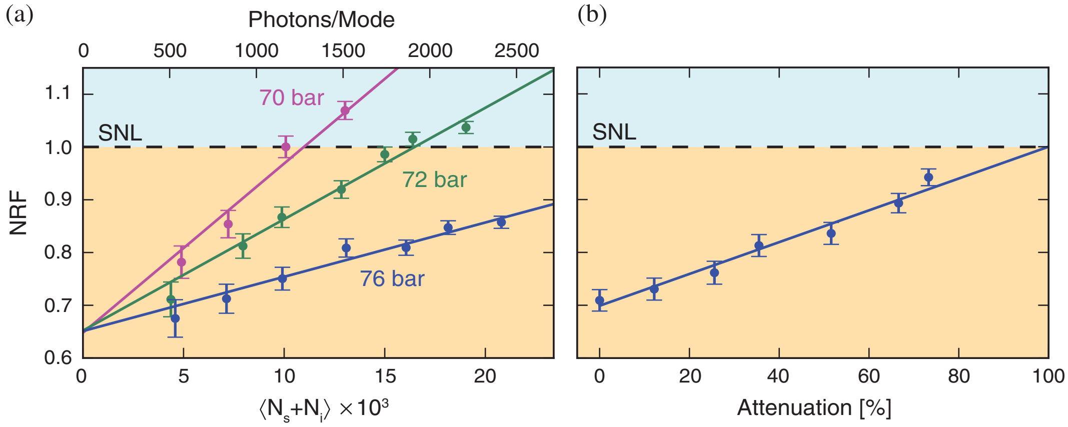

FIG. 3 (color). (a) NRF plotted against the average total number of twin-beam photons, changed by varying the pump power, at 70, 72, and 76 bar. The difference in slope is caused by unequal frequency dependence of the detection efficiency in the two optical channels (the sideband frequencies shift when the pressure is changed). (b) Measured values of NRF plotted against attenuation in the optical channel performed with the HWP and the PBS. Each data point in the diagram corresponds to one million recorded pulses. Error bars represent the standard error of the measurement.

loss in the system, e.g., the loss of the kagome-PCF (lowest loss reported at 800 nm is 70 dB/km [36]). With such state-of-the-art PCF and antireflection-coated gas-cell windows, the source itself would introduce a total loss of ~1.5%. This would correspond to an optimal NRF of −18 dB; all other losses relate to the detection scheme and are the same for any source.

We determined the effective number of spatiotemporal modes K in the system by measuring the second-order intensity correlation function $g^{(2)}$ (see Supplemental Material [24], Sec. 5) [37], corresponding to the product of effective spatial and temporal mode numbers. Here, we measured $g^{(2)} = 1.232 \pm 0.014$, which leads to $K = 4.31 \pm 0.26$. By inserting a 10 nm bandpass filter centered at 960 nm into the long-wavelength channel, the correlation time of the intensity fluctuations was increased, allowing us to measure only the number of spatial modes, which turned out to be 1. This means that the measured number of modes is equal to the effective number of temporal modes. The spatially single-mode behavior, confirmed by near-field imaging [Fig. 1(b)], together with the extraordinarily low number of temporal modes, make this system extremely interesting for quantum optical metrology. Comparable sources of nonclassical light based on bulk crystals usually emit at least 400 modes [38].

In conclusion, noble-gas-filled hollow-core kagome PCF is ideal for creating ultrafast photon-number-correlated twin-beam SV. The central sideband frequency can be tuned over ~80 THz by simply changing the gas pressure. Technical limitations, like the dropping QE of the photodiode, prevented us from measuring noise reduction over the whole tuning range. However, there is no fundamental physical reason restricting the usable spectral tuning range of the source. The absence of SpRS means that photon-number correlated sidebands can be efficiently generated close to the pump wavelength, unlike in solid-core glass fibers. As a result, femtosecond signal and idler pulses can be generated along the whole length of the fiber, without significant group velocity walk-off. This opens up additional possibilities for ultrafast quantum optics using fiber sources. Furthermore, the very broad spectral bandwidth of ~50 THz makes the system highly interesting for spectroscopic applications. Also remarkable is the low (<5) number of temporal modes of the spatial single mode system. The measured twin-beam squeezing of ~35% below the shot-noise level is mainly limited by the losses in the PCF itself and in the optical channels after the PCF. Photon-number correlation has been achieved for a squeezed vacuum state with a record brightness of ~2500 photons per mode. The system overcomes many of the material restrictions of solid-state systems and has the potential to push twin-beam generation into the UV. In the future, it should be possible to tailor the kagome-PCF dispersion to the pump laser, permitting a further reduction in the number of temporal modes and allowing realization of a Raman-free single spatiotemporal mode source of twin beams.

The research received partial financial support from the EU FP7 under Grant Agreement No. 308803 (Project BRISQ2).

*martin.finger@mpl.mpg.de
†Present address: Department of Physics, Technical University of Denmark, Fysikvej Building 309, 2800 Kgs. Lyngby, Denmark.

[1] V. Giovannetti, S. Lloyd, and L. Maccone, Quantum-enhanced measurements: Beating the standard quantum limit, Science **306**, 1330 (2004).
[2] N. Treps, U. Andersen, B. Buchler, P. K. Lam, A. Maître, H.-A. Bachor, and C. Fabre, Surpassing the Standard

Quantum Limit for Optical Imaging Using Nonclassical Multimode Light, Phys. Rev. Lett. **88**, 203601 (2002).
[3] P. Anisimov, G. M. Raterman, A. Chiruvelli, W. N. Plick, S. D. Huver, H. Lee, and J. P. Dowling, Quantum Metrology with Two-Mode Squeezed Vacuum: Parity Detection Beats the Heisenberg Limit, Phys. Rev. Lett. **104**, 103602 (2010).
[4] F. Hudelist, J. Kong, C. Liu, J. Jing, Z. Y. Ou, and W. Zhang, Quantum metrology with parametric amplifier-based photon correlation interferometers, Nat. Commun. **5**, 3049 (2014).
[5] A. Gatti, E. Brambilla, and L. A. Lugiato, Quantum Entangled Images, Phys. Rev. Lett. **83**, 1763 (1999).
[6] G. Brida, M. Genovese, and I. R. Berchera, Experimental realization of sub-shot-noise quantum imaging, Nat. Photonics **4**, 227 (2010).
[7] E. D. Lopaeva, I. R. Berchera, I. P. Degiovanni, S. Olivares, G. Brida, and M. Genovese, Experimental Realization of Quantum Illumination, Phys. Rev. Lett. **110**, 153603 (2013).
[8] N. Gisin, G. Ribordy, W. Tittel, and H. Zbinden, Quantum cryptography, Rev. Mod. Phys. **74**, 145 (2002).
[9] D. C. Burnham and D. L. Weinberg, Observation of Simultaneity in Parametric Production of Optical Photon Pairs, Phys. Rev. Lett. **25**, 84 (1970).
[10] O. Jedrkiewicz, Y.-K. Jiang, E. Brambilla, A. Gatti, M. Bache, L. A. Lugiato, and P. Di Trapani, Detection of Sub-Shot-Noise Spatial Correlation in High-Gain Parametric Down Conversion, Phys. Rev. Lett. **93**, 243601 (2004).
[11] I. N. Agafonov, M. V. Chekhova, and G. Leuchs, Two-color bright squeezed vacuum, Phys. Rev. A **82**, 011801(R) (2010).
[12] K. Garay-Palmett, H. J. McGuinness, O. Cohen, J. S. Lundeen, R. Rangel-Rojo, A. B. U'Ren, M. G. Raymer, C. J. McKinstrie, S. Radic, and I. A. Walmsley, Photon pair-state preparation with tailored spectral properties by spontaneous four-wave mixing in photonic-crystal fiber, Opt. Express **15**, 14870 (2007).
[13] N. J. Cerf, M. Bourennane, A. Karlsson, and N. Gisin, Security of Quantum Key Distribution Using *d*-Level Systems, Phys. Rev. Lett. **88**, 127902 (2002).
[14] J. T. Barreiro, T.-C. Wei, and P. G. Kwiat, Beating the channel capacity limit for linear photonic superdense coding, Nat. Phys. **4**, 282 (2008).
[15] B. Brecht, A. Eckstein, A. Christ, H. Suche, and C. Silberhorn, From quantum pulse gate to quantum pulse shaper–engineered frequency conversion in nonlinear optical waveguides, New J. Phys. **13**, 065029 (2011).
[16] B. Brecht, A. Eckstein, R. Ricken, V. Quiring, H. Suche, L. Sansoni, and C. Silberhorn, Demonstration of coherent time-frequency Schmidt mode selection using dispersion-engineered frequency conversion, Phys. Rev. A **90**, 030302 (2014).
[17] J. Fan, A. Migdall, and L. Wang, A twin photon source, Opt. Photonics News **18**, 26 (2007).
[18] J. G. Rarity, J. Fulconis, J. Duligall, W. J. Wadsworth, and P. St. J. Russell, Photonic crystal fiber source of correlated photon pairs, Opt. Express **13**, 534 (2005).
[19] B. J. Smith, P. Mahou, O. Cohen, J. S. Lundeen, and I. A. Walmsley, Photon pair generation in birefringent optical fibers, Opt. Express **17**, 23589 (2009).
[20] J. E. Sharping, J. Chen, X. Li, and P. Kumar, Quantum correlated twin photons from microstructure fiber, Opt. Express **12**, 3086 (2004).
[21] S. Dyer, B. Baek, and S. Nam, High-brightness, low-noise, all-fiber photon pair source, Opt. Express **17**, 10290 (2009).
[22] Q. Lin and G. P. Agrawal, Silicon waveguides for creating quantum-correlated photon pairs, Opt. Lett. **31**, 3140 (2006).
[23] G. P. Agrawal, *Nonlinear Fiber Optics*, 3rd ed. (Academic Press San Diego, 2001).
[24] See Supplemental Material at http://link.aps.org/supplemental/10.1103/PhysRevLett.115.143602 for the derivation of the FWM Hamiltonian and the measurement of the power dependence of the sidebands and the calibration of the shot-noise level. Furthermore, it includes an estimation of the loss in the optical channel and the derivation of the relation between g(2) and the effective number of modes, which includes Refs. [25–28].
[25] D. N. Klyshko, *Photons and Nonlinear Optics* (Gordon and Breach Science Publishers, New York, 1988).
[26] J. Chen, K. F. Lee, and P. Kumar, Quantum theory of degenerate $x^{(3)}$ two-photon statearXiv:quant-ph/0702176.
[27] C. K. Law, I. A. Walmsley, and J. H. Eberly, Continuous frequency entanglement: Effective finite Hilbert space and entropy control, Phys. Rev. Lett. **84**, 5304 (2000).
[28] P. Sharapova, A. M. Pérez, O. V. Tikhonova, and M. V. Chekhova, Schmidt modes in the angular spectrum of bright squeezed vacuum, Phys. Rev. A **91**, 043816 (2015).
[29] L. Mandel and E. Wolf, *Optical Coherence and Quantum Optics* (Cambridge University Press, Cambridge, England, 1995).
[30] L. J. Wang, C. K. Hong, and S. R. Friberg, Generation of correlated photons via four-wave mixing in optical fibers, J. Opt. B **3**, 346 (2001).
[31] J. C. Travers, W. Chang, J. Nold, N. Y. Joly, and P. St. J. Russell, Ultrafast nonlinear optics in gas-filled hollow-core photonic crystal fibers, J. Opt. Soc. Am. B **28**, A11 (2011).
[32] J. Nold, P. Hölzer, N. Y. Joly, G. K. L. Wong, A. Nazarkin, A. Podlipensky, M. Scharrer, and P. St. J. Russell, Pressure-controlled phase matching to third harmonic in Ar-filled hollow-core photonic crystal fiber, Opt. Lett. **35**, 2922 (2010).
[33] M. A. Finger, N. Y. Joly, T. Weiss, and P. St. J. Russell, Accuracy of the capillary approximation for gas-filled kagome-style photonic crystal fibers, Opt. Lett. **39**, 821 (2014).
[34] O. Aytür and P. Kumar, Pulsed twin beams of light, Phys. Rev. Lett. **65**, 1551 (1990).
[35] I. N. Agafonov, M. V. Chekhova, T. S. Iskhakov, A. N. Penin, G. O. Rytikov, and O. A. Shcherbina, Absolute calibration of photodetectors: photocurrent multiplication versus photocurrent subtraction, Opt. Lett. **36**, 1329 (2011).
[36] T. D. Bradley, Y. Wang, M. Alharbi, B. Debord, C. Fourcade-Dutin, B. Beaudou, F. Gerome, and F. Benabid, Optical properties of low loss (70 dB/km) hypocycloid-core kagome hollow core photonic crystal fiber for Rb and Cs based optical applications, J. Lightwave Technol. **31**, 2752 (2013).
[37] A. Christ, K. Laiho, A. Eckstein, K. N. Cassemiro, and C. Silberhorn, Probing multimode squeezing with correlation functions, New J. Phys. **13**, 033027 (2011).
[38] A. M. Pérez, T. Sh. Iskhakov, P. Sharapova, S. Lemieux, O. V. Tikhonova, M. V. Chekhova, and G. Leuchs, Bright squeezed-vacuum source with 1.1 spatial mode, Opt. Lett. **39**, 2403 (2014).